ISSN 2320 2599
Volume 2, No.2, March – April 2013
International Journal of Microwaves Applications
Available Online at http://warse.org/pdfs/2013/ijma12222013.pdf

Microstrip Quasi-TEM Resonator for Magnetic Resonance Imaging at High Field of 8T

RACHID BOUHMIDI[1], NADIA BENABDALLAH[2], NASREDDINE BENAHMED[3] and FETHI TARIK BENDIMERAD[3]
[1]Department of Electronics, University of Saida, Algeria
[2]Department of Physics, Preparatory School of Sciences and Technology (EPST-Tlemcen), Tlemcen, Algeria
[3]Department of Telecommunications, University of Tlemcen, P. O. Box 119, (13000) Tlemcen, Algeria

ABSTRACT

In this work, we used the finite element method (FEM) and the multiconductor transmission lines (MTL) method for designing an UHF magnetic resonance imaging (MRI) probe. This radio frequency (RF) volume coil quasi-transverse electromagnetic (quasi-TEM) type, based on the use of 16 microstrip transmission line elements has been developed for in vivo hydrogen magnetic resonance (H^1MR) application on small animals at a field of 8T. The quasi-TEM resonator coil compared with the shielded birdcage coil is characterized major advantages: simple coil structure, high-quality factor and completely distributed circuit. The implemented numerical tool allows the determination of the primary parameters, matrices [L] and [C], and simulates the frequency response of the reflection coefficient of the RF excitation port of the resonator, which allows us to estimate the level of adaptation of this RF volume coil for imaging small animals at Larmor frequency of 340 MHz.

Keywords :UHF-MRI probe; microstrip quasi-TEM resonator; FEM method; electromagnetic parameters; resonant modes.

1. INTRODUCTION

The structures of the TEM resonator had their first descriptions in the patents [1, 2], then several articles have been published on the modeling TEM resonator subject [3, 4]. Vaughan et al have developed a model based on transmission lines [3]. Although the modeling performance of RF resonators in high magnetic fields requires a physical approach that goes beyond the conventional concepts of lumped circuits, Tropp has developed a lumped model circuit which operates at a relatively low frequency of 143 MHz [4]. Bogdanov et al have developed a TEM resonator model based on lumped circuits at the operating frequency of 200 MHz [5]. At higher frequencies this model becomes divergent. In this paper, the model of multiconductor transmission lines which includes the exact calculation of the primary parameters matrices is developed to efficiently design the behavior of the loaded TEM resonator (i.e quasi-TEM) at the Larmor frequency of 340 MHz.

2. THEORY

The quasi-TEM resonator is considered as a system of n+1 multiconductor transmission lines, the geometric and physical properties of the resonator are uniform in the z direction of propagation of currents and voltages. The relationship between the vector $\hat{I}$ of natural currents $\hat{i}_1.....\hat{i}_n$ and the vector $\hat{V}$ of natural tensions $\hat{v}_1.....\hat{v}_n$ are expressed by the Telegraphist equations:

$$\frac{d\hat{V}(z)}{dz} = -\hat{Z}\,\hat{I}(z) \quad (1.a)$$

$$\frac{d\hat{I}(z)}{dz} = -\hat{Y}\,\hat{V}(z) \quad (1.b)$$

Complex impedance and admittance matrices per unit length $\hat{Z}$, $\hat{Y}$ are symmetric and of order n. They are also formed by symmetric and real matrices of order n: resistance R, inductance L, capacitance C and conductance G, so that:

$$\hat{Z} = R + jL\omega \quad (2.a)$$

$$\hat{Y} = G + jC\omega \quad (2.b)$$

Where ω is the angular frequency.

The matrices L, C and G are positive definite and can be determined by energy considerations. The fundamental assumption for the determination of these matrices is that the distribution of the electromagnetic field is larger in the orthogonal plane to the length of the resonator. Under this quasi-TEM condition electromagnetic field distribution is identical to that resulting from static excitation of the resonator, which allows the determination of the matrices L, C and G from the solution of Laplace's equation in the transverse plane of the resonator [6-9]. In the case where n+1 conductors are surrounded by a medium of conductivity σ, permittivity ε and permeability μ, then L, C and G are related by:

$$LC = CL = \mu\varepsilon\, I_n \quad (3.a)$$

$$LG = GL = \mu\sigma\, I_n \quad (3.b)$$

Where I_n is the identity matrix of order n.

The propagation equations of the natural currents and voltages are obtained from equations (1.a) and (1.b):

$$\frac{d^2\hat{V}(z)}{dz^2} = \hat{Z}\hat{Y}\,\hat{V}(z) \quad (4.a)$$

$$\frac{d^2\hat{I}(z)}{dz^2} = \hat{Y}\hat{Z}\,\hat{I}(z) \quad (4.b)$$

In equations (4.a) and (4.b) the product of matrices $\hat{Z}$ and $\hat{Y}$ is a full matrix, the voltage (current) on a conductor depends on the voltages (currents) on the other conductors, the

solution of these equations goes through a suitable diagonalization of matrices $\hat{Z}\hat{Y}$ and $\hat{Y}\hat{Z}$ [10, 11]. The change of variables leading to the diagonalization is given by:

$$\hat{V}(z) = \hat{T}_V \hat{V}_m(z) \tag{5.a}$$

$$\hat{I}(z) = \hat{T}_I \hat{I}_m(z) \tag{5.b}$$

Matrices $\hat{T}_V$ and $\hat{T}_I$ express the passage of the natural current $\hat{I}(z)$ and voltage $\hat{V}(z)$ vectors to current and voltage eigenvectors which define the modes of propagation. Substituting the transformation given in (5.a) and (5.b) in equations (4.a) and (4.b) we have:

$$\frac{d^2 \hat{V}_m(z)}{dz^2} = \hat{T}_V \hat{Z}\hat{Y} \hat{T}_V \hat{V}_m(z) \tag{6.a}$$

$$\frac{d^2 \hat{I}_m(z)}{dz^2} = \hat{T}_I \hat{Y}\hat{Z} \hat{T}_I \hat{I}_m(z) \tag{6.b}$$

The solution of equations (6.a) and (6.b) amounts to finding matrices $\hat{T}_V$ and $\hat{T}_I$ such that:

$$\hat{T}_V \hat{Z}\hat{Y} \hat{T}_V = \left[\hat{\gamma}^2\right] \tag{7.a}$$

$$\hat{T}_I \hat{Y}\hat{Z} \hat{T}_I = \left[\hat{\gamma}^2\right] \tag{7.b}$$

Where $\left[\hat{\gamma}^2\right] = diag(\hat{\gamma}_1^2 .....\hat{\gamma}_n^2)$ is a diagonal matrix containing the eigen values $\hat{\gamma}_1^2 .....\hat{\gamma}_n^2$ corresponding to the propagation constants of different modes. The determination of the eigenvectors $\hat{T}_{V_k}$ and $\hat{T}_{I_k}$ and eigen values $\hat{\gamma}_k^2$ (k = 1……. n) leads to the solutions of equations (6.a) and (6.b), which leads to:

$$\hat{V}(z) = \hat{T}_V (e^{-\hat{\gamma}z}\hat{V}_m^+ + e^{+\hat{\gamma}z}\hat{V}_m^-) \tag{8.a}$$

$$\hat{I}(z) = \hat{T}_I (e^{-\hat{\gamma}z}\hat{I}_m^+ - e^{+\hat{\gamma}z}\hat{I}_m^-) \tag{8.b}$$

The general solution (8.a) and (8.b) contains 4n unknowns in the vector $\hat{V}_m^+$, $\hat{V}_m^-$, $\hat{I}_m^+$ and $\hat{I}_m^-$ of size n. The number of unknowns can be reduced to 2n by substituting (8a) in (1b):

$$\hat{V}(z) = -\hat{Y}^{-1} \frac{d\,\hat{I}(z)}{dz}$$

$$\hat{V}(z) = \hat{Y}^{-1}\hat{T}_I \gamma \hat{T}_I^{-1}\hat{T}_I (e^{-\hat{\gamma}z}\hat{I}_m^+ - e^{+\hat{\gamma}z}\hat{I}_m^-) \tag{9}$$

A characteristic impedance matrix is defined as [10]:

$$\hat{Z}_c = \hat{Y}^{-1}\hat{T}_I \gamma \hat{T}_I^{-1} \tag{10}$$

then:

$$\hat{V}(z) = \hat{Z}_c \hat{T}_I (e^{-\hat{\gamma}z}\hat{I}_m^+ - e^{+\hat{\gamma}z}\hat{I}_m^-) \tag{11.a}$$

$$\hat{I}(z) = \hat{T}_I (e^{-\hat{\gamma}z}\hat{I}_m^+ - e^{+\hat{\gamma}z}\hat{I}_m^-) \tag{11.b}$$

The solution is completed by the determination of the incident and reflected current amplitudes vectors $\hat{I}_m^+$, $\hat{I}_m^-$. These vectors are determined by the boundary conditions imposed at the point of abscissa $z = 0$ and $z = l$ (l is the length of the resonator). The network of passive loads $\hat{Z}_S$ and sources $\hat{V}_S$ connected to the end z = 0 of the resonator will provide n equations relating the n tensions $\hat{V}(0)$ to the n current $\hat{I}(0)$ while the passive charges network $\hat{Z}_L$ and possible sources $\hat{V}_L$ connected to the end $z = l$ of the resonator provide n equations relating the n tensions $\hat{V}(l)$ to the n current $\hat{I}(l)$:

$$\hat{V}(0) = \hat{V}_S - \hat{Z}_S \hat{I}(0) \tag{12.a}$$

$$\hat{V}(l) = \hat{V}_L - \hat{Z}_L \hat{I}(l) \tag{12.b}$$

The application of boundary conditions (12.a) and (12.b) to equations (11.a) and (11.b) allows expressing the natural currents and voltages at any point z along the coupled lines of the resonator using the chain matrix:

$$\begin{bmatrix} \hat{V}(z) \\ \hat{I}(z) \end{bmatrix} = \begin{bmatrix} \hat{\Phi}_{11}(z) & \hat{\Phi}_{12}(z) \\ \hat{\Phi}_{21}(z) & \hat{\Phi}_{22}(z) \end{bmatrix} \begin{bmatrix} \hat{V}(0) \\ \hat{I}(0) \end{bmatrix} \tag{13}$$

Evaluation of natural currents and voltages at the points of abscissa $z = 0$ and $z = l$ and the elimination of the of incident and reflected wave amplitudes currents $\hat{I}_m^{\pm}$, gives the expressions of the sub matrices:

$$\hat{\Phi}_{11}(l) = \hat{Z}_c \hat{T}_I \cosh(\gamma l)\hat{T}_I^{-1}\hat{Y}_c \tag{14.a}$$

$$\hat{\Phi}_{12}(l) = -\hat{Z}_c \hat{T}_I \sinh(\gamma l)\hat{T}_I^{-1} \tag{14.b}$$

$$\hat{\Phi}_{21}(l) = -\hat{T}_I \sinh(\gamma l)\hat{T}_I^{-1}\hat{Y}_c \tag{14.c}$$

$$\hat{\Phi}_{22}(l) = \hat{T}_I \cosh(\gamma l)\hat{T}_I^{-1} \tag{14.d}$$

Once the chain matrix formed the input impedance matrix of the resonator can be calculated taking into account the absence of sources at the end $z = l$ of the resonator:

$$\hat{Z}_{in} = \frac{\hat{V}(0)}{\hat{I}(0)} = \frac{(\hat{Z}_L \hat{\Phi}_{22}(l) - \hat{\Phi}_{12}(l))}{(\hat{\Phi}_{11}(l) - \hat{Z}_L \hat{\Phi}_{21}(l))} \tag{15}$$

By having the input impedance matrix (15), the quasi-TEM resonator and the network connected to the end $z = 0$ are simulated as a lumped circuit [4, 5]. The current delivered by the RF source allows the calculation of the input impedance z_{in} and reflection coefficient S_{11} seen by this RF source [11]:

$$z_{in} = \frac{v_S}{i_S} - R_S \tag{16}$$

$$S_{11} = \frac{z_{in} - R_S}{z_{in} + R_S} \tag{17}$$

Where R_S is the impedance of the RF source and the power cable, typically equal to 50Ω.

3. RESULTS

The quasi-TEM resonator schematically shown in figure 1-a consists of 16 microstrip conductors 0.64 cm wide and 38 μm thick. These microstrips are arranged on the inside of a plexiglas

cylinder 7.25 cm in diameter, the outer surface of the cylinder diameter of 10.5 cm is completely covered with copper of thickness 38 μm and is the ground plane. The plexiglas material used in the design has a relative dielectric constant (ε_r) 3.3 at interest frequency (340 MHz).The length of the resonator is comparatively sized with respect to the wavelength in free space λ_0, $l = 0.177\ \lambda_0$.

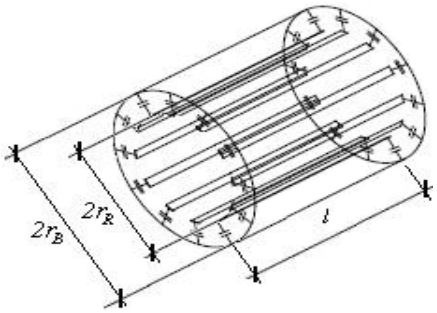

a)

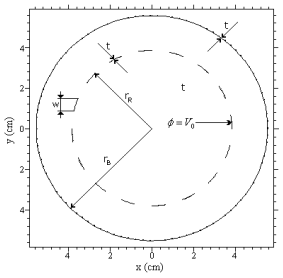

b)

Figure 1: (a) Schematic of the quasi-TEM resonator, (b) Structure with the boundary conditions specified for the potential.

3.1 Evaluation of the primary electromagnetic (EM) parameters

Using our FEM approach under FreeFEM environment [12], the primary parameters matrices per unit length of the quasi-TEM resonator are obtained by solving the Laplace's equation:

$$\nabla_t(\varepsilon \nabla_t \phi) = 0 \tag{18}$$

$\phi = V_0$ on the $i^{ème}$ conductor and $\phi = 0$ on all other conductors.

The geometric structure of the resonator and the boundary conditions on the electrical potential ϕ set for conductors are shown in figure 1-b.

The finite element method (FEM) is used to solve the equation (18). Figure 2.a shows triangular FEM-meshes of the resonator and the electrical potential ϕ is estimated at the vertices of triangles from the boundary conditions defined for the structure, figure 2.b shows the obtained distribution of electric potential inside the resonator.

The calculation of electric potential on the orthogonal plane to the length of the resonator allows the determination of the first line of capacitance C.

$$C_{i,j} = -\frac{1}{V_0}\int_{l_j} \varepsilon \frac{\partial \phi}{\partial n} \tag{19}$$

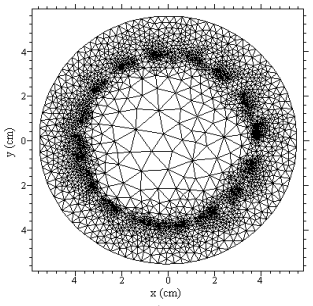

a)

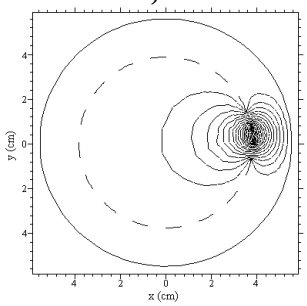

b)

Figure 2: (a) FEM-Meshes of the structure, (b) Distribution of the potential.

Solving the Laplace equation by replacing all dielectrics with air provides the capacity matrix C_0, the matrix inductance matrices L is expressed by:

$$L_{i,j} = \mu_0 \varepsilon_0 C_{0i,j} \tag{20}$$

Table 1 lists the first column of the matrices C, C_0 and L obtained by the FEM method. This information is sufficient to reconstruct the complete matrices since they are circulant [6-9].

Table 1. EM parameters of the MRI resonator.

Colonne	C (pF/m)	C_0 (pF/m)	L (nH/m)
1	52.180	23.363	0.557
2	-10.270	-5.529	0.158
3	-0.984	-0.804	0.070
4	-0.315	-0.323	0.039
5	-0.179	-0.191	0.025
6	-0.127	-0.136	0.019
7	-0.101	-0.109	0.015
8	-0.090	-0.097	0.014
9	-0.086	-0.093	0.013
10	-0.090	-0.097	0.014
11	-0.101	-0.109	0.015
12	-0.127	-0.136	0.019
13	-0.179	-0.191	0.025
14	-0.315	-0.323	0.039
15	-0.984	-0.804	0.070
16	-10.270	-5.529	0.158

3.2 Multiconductor transmission lines model predictions

When the primary EM parameters are numerically determined, it is possible to estimate the resonance spectrum S_{11} of the resonator shown in figure 3 using our programs.

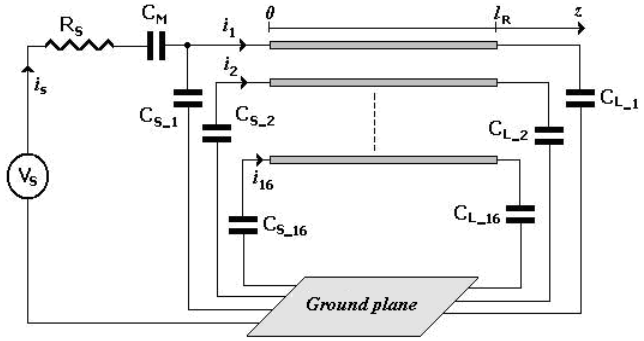

Figure 3: Schematic circuit of the quasi-TEM UHF-MRI probe.

The simulated model is excited by an RF voltage source of impedance 50 Ω. This model is adjusted so that the mode of interest occurs at a frequency of 340 MHz, this is achieved by adjusting capacitors $C_{L\text{-}n}$ and $C_{S\text{-}n}$ (n = 1,...,16) connected at the ends of the resonator at 1.85 pF. As shown in figure 4, a level of reflection of 93.86 dB is obtained by adjusting the adaptation capacitor C_M to 5.98 pF.

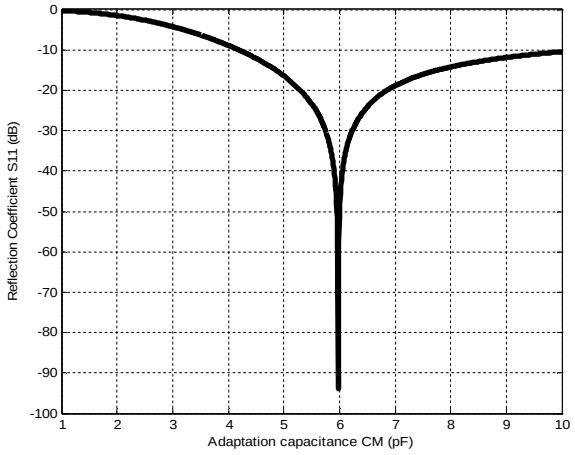

Figure 4: Sizing of the adaptation capacitor of the UHF-MRI probe.

The simulated frequency response of S_{11} at the RF port of our designed UHF-MRI probe is shown in figure 5. The curve presents a minimum at the chosen resonant frequency, i.e., 340 MHz. The obtained minimum of reflection for the quasi-TEM resonator is very low (-93.86 dB) at the resonance frequency.

The resonance frequencies and levels of reflection associated to the eight resonant modes are listed in table 2.

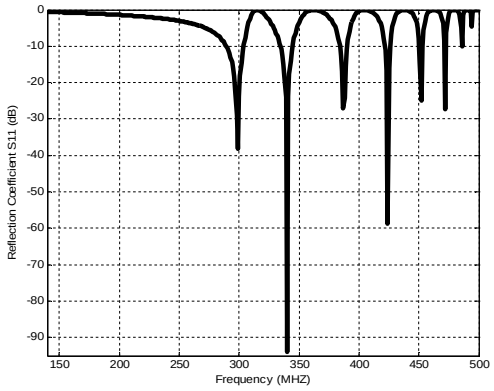

Figure 5: Reverse transmission, S_{11}, at the RF port of our designed UHF-MRI resonator.

Table 2. Resonant modes of the quasi-TEM UHF-MRI resonator.

Modes	Frequency (MHz)	S_{11} (dB)
0	299	-38.22
1	340	-93. 86
2	387	-27.17
3	424	-58.78
4	452	-24.98
5	472	-27.36
6	486	-10.12
7	494	-04.68

3.3 Comparison with the lumped circuit model

To validate the model of multiconductor transmission lines, an equivalent lumped circuit model is developed for comparison. In this model the coupled transmission lines resonator are treated as inductors with mutual coupling between them. The equivalent lumped circuit of the quasi-TEM probe is shown in figure 6, while figure 7 shows the frequency response which we obtained for this circuit.

For the first mode, the circuit has a minimum of reflection of -27.63 dB obtained at the resonant frequency of 363 MHz. From figures 5 and 7, it appears clearly that multiconductor transmission lines model is adapted to design quasi-TEM UHF-MRI probes more than lumped circuit model.

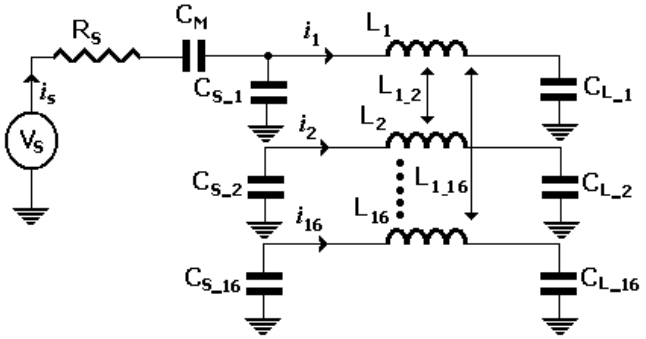

Figure 6: Lumped circuit model of the quasi-TEM UHF-MRI probe.

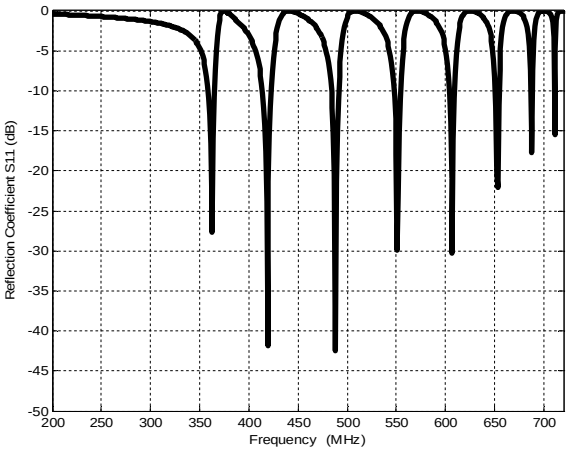

Figure 7: Frequency response of the quasi-TEM resonator using lumped elements.

4. CONCLUSION

In this paper the multiconductor transmission lines model has been developed and successfully implemented to analyze and design a 16 microstrip lines quasi-TEM resonator for small animal imaging at 8T.

The multiconductor transmission lines model has been applied to a system of small dimension, its theoretical foundations and implementations allow evaluating the resonance spectrum of the UHF-MRI resonator.

The resonant frequency of mode 1 can be adjusted by means of end capacitors while the level of adaptation of the resonator is adjusted by means of the capacitor fed by the RF source.

The simulation of the frequency response of the model in lumped circuits shows a considerable discrepancy with that of the multiconductor transmission lines model, which allows us to confirm the usefulness of the distributed model.

REFERENCES

1. P. Röschmann, High-frequency coil system for a magnetic resonance imaging apparratus , US patent 4746866, 1988.
2. JF. Bridges, Cavity resonator with improved magnetic field uniformity for high frequency operation and reduced dielectric heating in NMR imaging devices, US patent 4751464, 1988.
3. JT. Vaughan, HP. Hetherrington, JO. Out, JW. Pan, GM. Pohost, "High frequency volume coils for clinical NMR imaging and spectroscopy," Magn Reson Med, Vol 32, 1994, pp. 206-218.
4. J. Tropp, "Mutual inductance in the birdcage resonator," Journal Magnetic Resonance, 1997.
5. G. Bogdanov, R. Ludwig, "A Coupled microstrip line transverse electromagnetic resonator model for high-field magnetic resonance imaging," Magnetic Resonance in Medicine, Vol. 47, 2002, pp. 579-593.
6. R. P. Clayton, "Decoupling the multiconductor transmission lines equations," IEEE Trans. Microwave Theory and Techniques., Vol. 44, no. 8, 1996, pp. 1429-1440.
7. N. Ben Ahmed, M. Feham, M. Khelif, "Analysis and design of a coupled coaxial line TEM resonator for magnetic resonance imaging," Journal of Physics in Medicine and Biology, Vol. 51, 2006, pp. 2093-2099.
8. R. Bouhmidi, N. Benabdallah, N. Ben Ahmed, M. Khelif, "Design coupled microstrip resonator for MRI," Microwave Journal, Vol. 46, 2007, pp. 59-66.
9. N. Benabdallah, N. Ben Ahmed, F. T. Bendimerad and K. Aliane, "Analysis and design of a 12-element-coupled-microstrip-line TEM resonator for MRI," International Journal of Microwaves Applications, Vol. 1, no.1, 2012, pp. 01-04.
10. R. P. Clayton, Analysis of multiconductor transmission lines, New York: John Wiley; 2008.
11. D. Pozar, Microwave engineering, New York: John Wiley; 1998.
12. www.FreeFEM.org